Vesicle capture on patterned surfaces coated with amphiphilic biopolymers

Matthew B. Dowling,[a] Vishal Javvaji,[bc] Gregory F. Payne*[ac] and Srinivasa R. Raghavan*[ab]

Received 16th August 2010, Accepted 10th November 2010
DOI: 10.1039/c0sm00825g

We describe a simple way to create patterns of "soft" biomolecular nanostructures such as vesicles on "hard" surfaces such as gold. The key to our approach is the use of an amphiphilic biopolymer as an "interconnect" or tether. The polymer is hydrophobically modified chitosan (hm-chitosan), which is obtained by covalently attaching alkyl tails to the backbone of chitosan. We electrodeposit films of hm-chitosan onto microscale gold cathodes formed by lithography on a silicon wafer. Subsequently, the hm-chitosan films are used to spontaneously capture vesicles from solution; this is demonstrated both for surfactant as well as lipid vesicles (liposomes). Vesicles remain strongly bound to the hm-chitosan to a much greater extent than to native chitosan. This suggests that the mechanism for vesicle capture involves non-covalent binding of hydrophobes from hm-chitosan chains to the hydrophobic portions of vesicle bilayers. Importantly, the vesicles captured by hm-chitosan films are *intact*—this is shown both by direct visualization of captured vesicles (*via* optical and cryo-transmission electron microscopy) as well as through the capture and subsequent disruption of dye-filled vesicles. Various microscale patterns of immobilized vesicles are created and the vesicles are demonstrated to be capable of sensing a reporter molecule from the external solution.

1. Introduction

Vesicles (or liposomes) are self-assembled "nano-containers" formed by lipids or surfactants in aqueous solution.[1] These structures are ~100 nm in size and comprise an aqueous core and a lipid bilayer. The aqueous core can be used to encapsulate hydrophilic molecules such as drugs, proteins, or genes, while hydrophobic and amphiphilic substances can be integrated into vesicle bilayers.[1] Few, if any, other nanostructures demonstrate this level of versatility as carriers of useful payloads. Accordingly, vesicles have been explored and exploited for a myriad of applications, including targeted drug delivery, gene transfection, imaging agents, biosensors, food science, and cosmetics.[2]

Recently, there has been considerable interest into the capture of intact vesicles at precise locations on solid substrates.[3–14] The motivation for such studies includes: (a) fundamental aspects, *e.g.*, related to vesicles as biological models for adherent cells, as well as (b) applied aspects related to the fabrication of biosensors or modified biomaterials. For example, the internal volume of intact vesicles would be available for entrapping biomolecules, drugs, or fluorescent molecules, which could be useful for sensor and immunoassay applications. In addition, proteins embedded in vesicle bilayers are expected to more closely mimic their *in vivo* function compared to the same proteins in supported planar bilayers.[4,12] There is particular interest in creating "vesicle arrays" *via* the spatially controlled immobilization of vesicles, which could spawn a new generation of biomolecular assay tools.[4,9]

Previous attempts to capture intact vesicles with spatial precision have employed DNA tethering,[4–6] covalent binding to gold or polystyrene,[7,8] or biotin–streptavidin linking schemes.[10–12] These methods generally involve labor-intensive experimental procedures or expensive chemical labels. An alternate simpler approach is to use amphiphilic polymers bearing hydrophobic (lipophilic) moieties as tethers to bind either supported lipid bilayers or vesicles to surfaces.[13–18] This approach has been used to capture label-free vesicles on the commercially available Biacore L1 chip;[13,14] however, this approach does not offer significant spatial resolution. A greater level of spatial and temporal control over vesicle capture (*i.e.*, onto specific areas of a given surface at a given time) could be advantageous for many applications, including the creation of vesicle arrays.

In this study, we explore a simple and inexpensive method to capture vesicles onto solid surfaces with a high degree of spatiotemporal control. Our method exploits two sets of key results from our laboratories over the past several years. The first is the ability to electrodeposit the biopolymer chitosan onto patterned surfaces using electrical signals.[19–22] Chitosan is a widely available cationic biopolymer that has a pH-responsive character ($pK_a \approx 6.0$), *i.e.*, it transforms from a soluble to an insoluble form upon increasing the pH above about 6.5. Accordingly, chitosan films can be deposited onto cathode surfaces upon application of a current due to the high local pH near this electrode.[19–21] Here, we extend the electrodeposition scheme to a derivative of chitosan that is functionalized with hydrophobic tails (Fig. 1). We term this derivative as "hydrophobically modified chitosan", or hm-chitosan for short.[23] Previously, we have studied the interaction between hm-chitosan and vesicles in solution.[23–25] The key result was that the hydrophobes from this amphiphilic biopolymer tended to insert into the hydrophobic bilayers of vesicles, thus transforming the vesicle solution into a "vesicle gel", with the vesicles now serving as junction points in a network. Here, we show that the affinity

[a]*Fishell Department of Bioengineering, University of Maryland, College Park, MD, 20742-2111, USA. E-mail: sraghava@umd.edu*
[b]*Department of Chemical & Biomolecular Engineering, University of Maryland, College Park, MD, 20742-2111, USA*
[c]*Center for Biosystems Research, University of Maryland Biotechnology Institute, 5115 Plant Sciences Building, College Park, MD, 20742, USA. E-mail: payne@umbi.umd.edu*

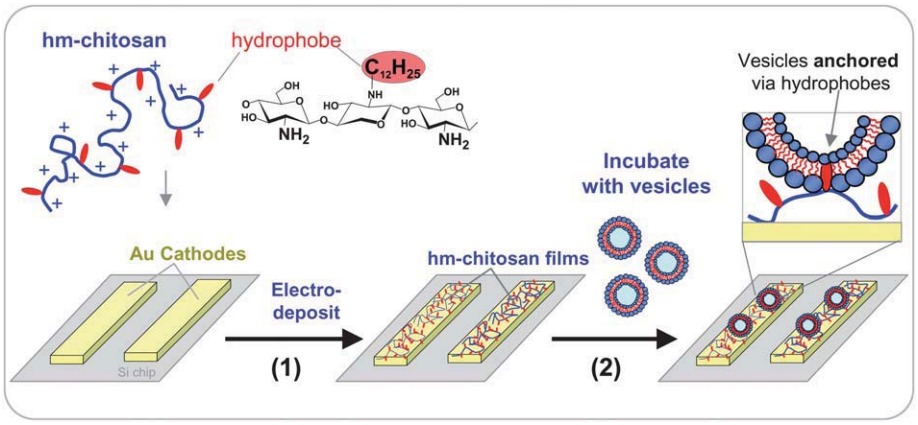

Fig. 1 Schematic showing the spatiotemporal capture of vesicles using hm-chitosan. The structure of hm-chitosan as well as a schematic of its chain are shown in the top left. The chain has a hydrophilic backbone shown in blue and pendant hydrophobes (C12 tails) that are shown in red. In step (1), thin films of hm-chitosan are electrodeposited onto gold cathodes that are patterned on a silicon chip. Next, in step (2), the chip is incubated with a solution of vesicles. Intact vesicles become spontaneously anchored onto the polymer films. The inset shows the likely mechanism for such anchoring, which is *via* non-covalent interaction between the hydrophobes on the polymer and vesicle bilayers.

for vesicles also extends to hm-chitosan films. When a surface coated with hm-chitosan is exposed to a solution of vesicles, *the film captures vesicles simply* via *non-covalent interactions between the vesicles and the polymer hydrophobes* (see schematic in Fig. 1). Thus, hm-chitosan can act as a "soft" interconnect or tether between vesicles and a hard surface such as a gold electrode.[22] Moreover, our ability to selectively deposit hm-chitosan in pre-designed patterns, as illustrated in Fig. 1, allows us to create corresponding patterns of immobilized vesicles.

It is worth emphasizing certain features of our approach as well as some potential applications. Our approach (Fig. 1) involves deposition of hm-chitosan followed by capture of vesicles on the surfaces of these films. The advantage is that the vesicles remain accessible to the external environment, which facilitates their use as sensors. (The accessibility of vesicles is more problematic if the vesicles are simply co-deposited with the polymer, as has been done earlier.[26]) We will also present several pieces of evidence to show that the vesicles are indeed intact, *i.e.*, they are not being ruptured into flat lipid bilayers within the hm-chitosan film. Thus, the payload within the vesicles is expected to remain available for future use. The latter aspect is important in considering potential applications for vesicle–polymer hybrid films in drug delivery or wound healing. For example, in the case of chronic-wound healing, macroscopic films of hm-chitosan could be therapeutically functionalized with vesicles housing several types of growth factors (*i.e.*, proteins that promote wound healing). These films could then be used to cover chronic wounds while protecting them from exudation or infection (chitosan is known also for its anti-bacterial properties). In turn, the controlled release of the growth factors from the vesicles attached to the films would enhance and sustain the wound-healing process. Note also that the bioactivity of growth factors is likely to be maintained when they are within vesicles; in contrast, growth factors embedded directly within polymer films may lose some of their activity.[27] In sum, vesicle–polymer hybrids can have interesting applications, and the present study shows how these materials can be readily assembled *via* non-covalent hydrophobic interactions.

2. Experimental section

Materials

Chitosan of medium molecular weight (190–310 K) and Brookfield viscosity of 286 cps was obtained from Sigma-Aldrich. The reported degree of deacetylation was about 80%. Chitosan is soluble only under acidic conditions (pH < 6.5) and here it was dissolved in 0.2 M acetic acid. The phospholipids L-α-phosphatidylcholine (PC) and biotinylated phosphatidylethanolamine (PE–biot), and the fluorescent lipid 1′-dioctadecyl-3,3,3′,3′-tetramethylindocarbocyanine perchlorate (DiI) were purchased from Avanti Polar Lipids. The surfactants cetyltrimethylammonium tosylate (CTAT), sodium dodecyl benzenesulfonate (SDBS), and Triton X-100, the dye 5,6-carboxyfluorescein (CF), and the reagent *n*-dodecyl aldehyde were purchased from Sigma-Aldrich. Streptavidin bound to fluorescein isothiocyanate (FITC–streptavidin) and the succinimidyl ester of CF (NHS–fluorescein) were purchased from Fluka. All experiments were performed using distilled-deionized (DI) water.

Synthesis of chitosan derivatives

The hm-chitosan was synthesized by attaching *n*-dodecyl tails to the chitosan backbone *via* reaction with *n*-dodecyl aldehyde. The procedure has been reported in our earlier paper[23] and follows that described in the literature.[28–30] The degree of hydrophobic substitution follows the reaction stoichiometry and in this study it was fixed at *ca.* 2.5 mol% of the available amine groups. Fluorescently labeled chitosan and hm-chitosan were synthesized by reacting the polymers with NHS–fluorescein, as previously reported in the literature.[20]

Vesicle and liposome preparation

Both surfactant vesicles and lipid vesicles (liposomes) have been used in this study. Catanionic surfactant vesicles[31,32] were prepared by mixing 0.7 wt% of the cationic surfactant CTAT and

0.3 wt% of the anionic surfactant SDBS (~2 : 1 molar ratio) in DI water and gently stirring overnight. Dye-filled catanionic vesicles were prepared by combining 1 mM of CF with the CTAT/SDBS mixture, followed by separation of vesicles from free dye using a Sephadex G-50 column (from Roche). Liposomes were prepared by an extrusion method, as recommended by the manufacturer (Avanti Polar Lipids). Briefly, dried films of the lipids were hydrated under moderate stirring, freeze–thawed 5 times, and then passed through two double-stacked polycarbonate membrane filters (100 nm pores) using a Lipex pressurized extrusion system. Dye-filled liposomes were prepared in DI water from PC (20 mM) and CF (15 mM) and purified of free CF using the Sephadex G-50 column. Fluorescently labeled liposomes and vesicles were prepared in DI water by combining the lipid PC (13 mM) or the surfactants with trace amounts (13 μM) of the fluorescent lipid DiI. For the streptavidin binding assay, biotinylated liposomes were prepared by combining PC and PE–biotin in a molar ratio of 9 : 1, with a total lipid concentration of 1 wt%. Vesicle sizes in all cases were measured using a Photocor-FC dynamic light scattering (DLS) instrument.

Preparation of giant unilamellar vesicles (GUVs)

The GUVs were prepared by electroformation, as described in the literature.[33,34] The lipids (1 mg mL^{-1}) and DiI (7.7 μg mL^{-1}) were dissolved in chloroform. One drop of this solution (5 μL) was deposited onto the conducting side of an indium tin-oxide (ITO)-coated glass slide. The solvent was removed first under desiccation for 1 h and then freeze-drying for 3 h. A chamber was then made by creating an O-ring out of Seal-Ease and then pressing a second ITO-coated slide, conducting side facing downward, above the original slide (gap depth of 1 mm). The chamber was hydrated with a solution of 100 mM sucrose in DI water *via* an injection needle through the Seal-Ease; after injection, the needle was removed and the hole closed by Seal-Ease. Alligator clips were connected to both glass slides as well as the function generator (BK Precision 10 MHz Sweep/Function Generator 4017) *via* a BNC connector. An electric potential of AC 1.5 V at 10 Hz (corresponding electric field of 1500 V m^{-1}) was applied for 2 h at 55 °C; the frequency was then dropped to 1 Hz for an additional 50 min. In the process, GUVs were found to appear in the fluid in the chamber.

Electrodeposition

Electrodeposition was performed on "chips" fabricated from silicon wafers with deposited micropatterns of gold (Fig. 2). Fabrication procedures have been described in detail in our earlier papers.[19–21] Electrodeposition was performed by negatively biasing a specific lead on the chip while it was partially immersed in an aqueous solution containing 1 wt% of either chitosan or hm-chitosan at a pH ≈ 5. A DC power supply (model 6641C, Agilent Technologies) was used to supply a constant current to the chip and counter electrode over a 2 min period. Photomicrographs of fluorescent electrodeposited materials were taken by a fluorescence stereomicroscope (MZFLIII, Leica) equipped with a digital camera (Spot 32, Diagnostic Instruments). To observe CF or FITC fluorescence, the microscope was set with an excitation wavelength of 480 nm (bandwidth of 40 nm) and a long-pass emission filter at 510 nm. To observe DiI fluorescence, the filters were chosen with an excitation wavelength of 560 nm (bandwidth of 40 nm) and an emission filter of 610 nm. In all cases, Image J1.34S software from NIH was used to analyze images and quantify fluorescence intensity.

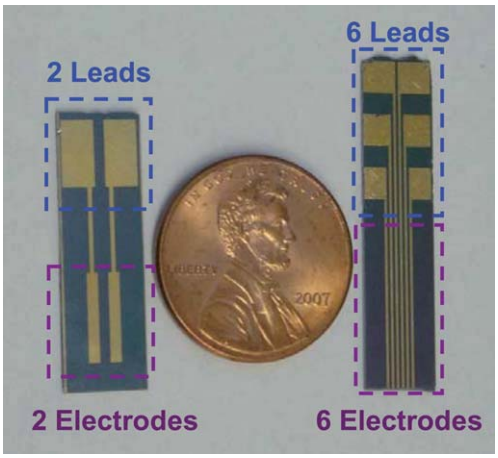

Fig. 2 Photograph of micropatterned chips used in this study. The leads and electrodes are formed by depositing gold on a silicon wafer using lithographic techniques. On the left is a 2-electrode chip and on the right a 6-electrode chip. A US penny is shown for size comparison.

Cryo-TEM

C-Flat holey carbon grids with a hole size of 1.2 μm were purchased from Electron Microscopy Sciences. Grids bearing hm-chitosan and surfactant vesicles were plunged into liquid ethane (−183 °C) using a Gatan CryoPlunge3, so as to form vitrified specimens and thereby preserve any molecular assemblies present. The samples were thereafter imaged on a JEOL-2100 LaB6 TEM at liquid nitrogen temperature.

3. Results and discussion

Vesicle capture on hm-chitosan films

The first step in our approach involves electrodeposition of hm-chitosan films onto gold electrodes. These films are then to be used to capture vesicles. In the context of vesicle capture, it is useful to compare hm-chitosan with the native chitosan (no hydrophobes). Electrodeposition of native chitosan was first demonstrated nearly a decade ago;[19] the present study is the first to extend this capability to hm-chitosan. For our initial studies, we used the two-electrode chip shown in Fig. 2. As mentioned earlier, the chip substrate is a silicon wafer, on which gold electrodes are deposited in a specific pattern. We then conducted sequential electrodeposition of hm-chitosan and chitosan (both tagged with the green fluorescent dye, NHS–fluorescein) on the left and right electrodes, respectively. This was done as follows: first, the right electrode was connected to the power supply and the other unconnected while the chip was immersed in a solution of chitosan. The connections were then switched (only left electrode connected) and the chip was immersed in a solution of hm-chitosan. After deposition, the electrodes were disconnected

from the power supply, and the chips were rinsed several times with DI water. Fig. 3 (top) shows the results of the experiment: the green color on both electrodes in the two fluorescence images indicates successful deposition of both hm-chitosan and chitosan.

Next we examined the relative capabilities of hm-chitosan and chitosan to capture vesicles from solution. These experiments were conducted with both surfactant vesicles as well as lipid vesicles (liposomes). The catanionic surfactant vesicles (70/30 CTAT/SDBS, total 1 wt%) had an average diameter around 120 nm, as measured by DLS. The liposomes of PC were made by extrusion through 100 nm membrane filters and had an average diameter around 110 nm from DLS. Both the vesicles and the liposomes were tagged with the fluorescent lipid DiI, which incorporates into the bilayer membranes of the above structures. Note that DiI exhibits a red fluorescence, *i.e.*, a distinct color compared to the green signal from the chitosan and hm-chitosan. We incubated the chip on the left with surfactant vesicles and the one on the right with the liposomes, both for 10 min. The chips were then rinsed three times with DI water to remove weakly adsorbed structures and then imaged under the fluorescence microscope using red filters. The resulting images (Fig. 3, bottom) show a significantly higher red fluorescent signal from the hm-chitosan side compared to the chitosan-side—and this is the case for both the surfactant vesicles and the liposomes. These results show that hm-chitosan is considerably more effective at capturing vesicles than chitosan. We believe this is because hydrophobes from hm-chitosan chains can get inserted into vesicle bilayers through non-covalent hydrophobic interactions (as depicted in Fig. 1). Such interactions enable a tight anchoring of the vesicles to the polymer film.

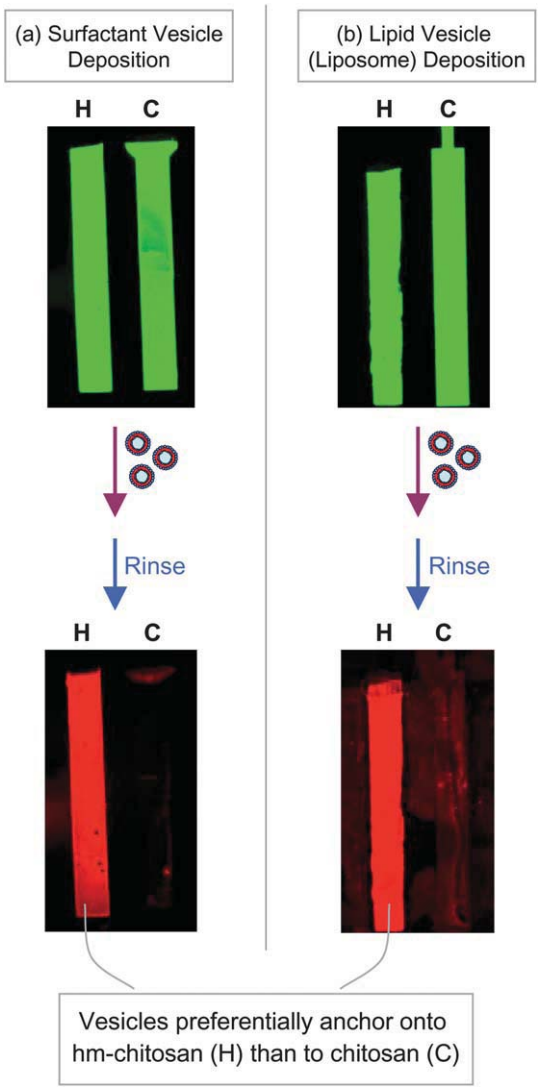

Fig. 3 Comparison of hm-chitosan (H) and chitosan (C) films in terms of their ability to capture vesicles. Top images: green-filtered fluorescence micrographs showing deposition of NHS-tagged hm-chitosan on the left electrode and NHS-tagged chitosan on the right electrode of a two-electrode chip. The chips are then incubated with vesicles for 10 min, followed by rinsing with DI water. Bottom images: red-filtered fluorescence micrographs showing the presence of DiI-tagged vesicles on the electrodes. The results in (a) (left-column) are obtained with catanionic surfactant vesicles, while those in (b) (right-column) are obtained with liposomes. In both cases, the stronger signals from the left electrodes indicate that vesicles are anchored preferentially to the hm-chitosan film than to the chitosan one.

The superior effectiveness of hm-chitosan in capturing vesicles is a robust result and this is further proven by experiments with varying vesicle incubation times. For these experiments, surfactant vesicles were used and the time of chip incubation in the vesicle solution was varied from 5 to 10 to 20 min. All other experimental variables, including rinsing times and image exposure time, were kept constant. The results in Fig. 4 show an increase in red fluorescence from the hm-chitosan electrode with increasing incubation time—the increase is quite significant between 5 and 10 min and slight between 10 and 20 min. In all cases, the signal from the hm-chitosan side dwarfs that from the

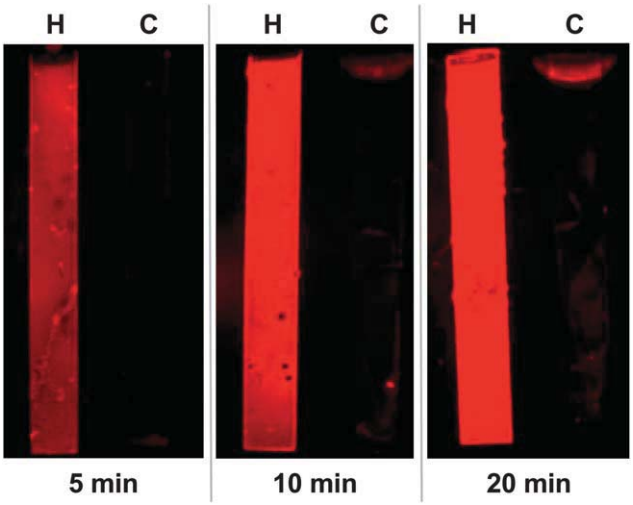

Fig. 4 Variation in the extent of vesicle capture based on the time of chip incubation with a vesicle solution. hm-Chitosan (H) and chitosan (C) are deposited on the left and right electrodes, respectively. The chip is incubated with a solution of surfactant vesicles for different lengths of time and then imaged by fluorescence microscopy. The images are red-filtered fluorescence micrographs showing DiI-tagged vesicles on the electrodes. A constant exposure time of 20 s at the excitation wavelength was used to obtain each image. The results show increasing capture of vesicles on the H side (increasing signal intensity) and negligible capture on the C side.

chitosan side. Similar results were obtained for macroscopic films of chitosan and hm-chitosan simply dried onto glass slides and incubated with tagged surfactant vesicles for various time intervals (data not shown). These results suggest that vesicle capture on hm-chitosan proceeds by surface diffusion of vesicles until they connect with free hydrophobes from the polymer, whereupon the vesicles get strongly bound.[5] As the free hydrophobes get used up, fewer vesicles are able to bind strongly and the binding capacity of the film becomes saturated.

Intactness of captured vesicles

Next we tackle the question of whether the vesicles captured on hm-chitosan films are intact or whether the red fluorescent signal reflects fragments of vesicle bilayers. Fig. 5 is a first piece of evidence to demonstrate the intactness of vesicles. In this case, we prepared a solution of fluorescently tagged giant unilamellar vesicles (GUVs) of phospholipids. Optical microscopy (not shown) revealed that the GUVs ranged in size from 10 to 50 μm, which is typical of GUVs made *via* electroformation. We then incubated a chip bearing hm-chitosan in the GUV solution for 10 min, rinsed the chip and observed it under a fluorescence microscope. Note the red fluorescent "hot spots" on the hm-chitosan film—these are shown at two different levels of magnification in Fig. 5. The spot sizes compare well with the sizes of GUVs and therefore it is likely that the spots correspond to intact GUVs. Thus, large microsized GUVs are shown to remain intact when immobilized on an hm-chitosan film.

Next, evidence for the intact capture of nanosized surfactant vesicles is provided by cryo-TEM. For these experiments, we deposited hm-chitosan directly on Holey-carbon TEM grids. These grids were then incubated with surfactant vesicles, followed by a rinsing step with DI water to remove weakly adsorbed vesicles. The rinsed grids were maintained in an aqueous environment at room temperature. These grids were then prepared in the usual way for cryo-TEM (see Experimental section) by plunging into liquid ethane. Observation of the vitrified specimens showed the presence of numerous spherical structures of 100–150 nm diameter (Fig. 6). These are evidently the surfactant

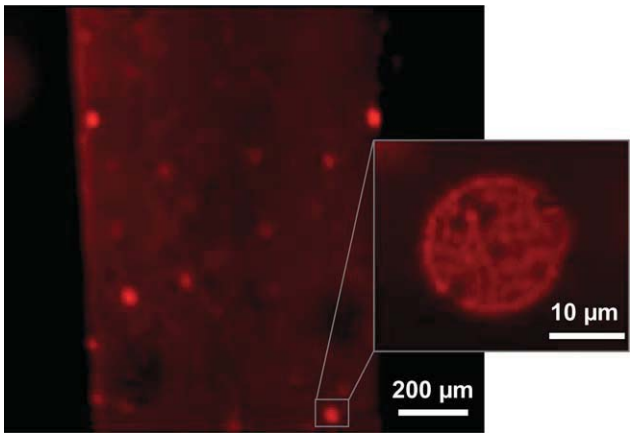

Fig. 5 Immobilization of giant unilamellar vesicles (GUVs) on an hm-chitosan film. After 10 min incubation with DiI-tagged GUVs, multiple red-fluorescent 'hot spots' appear on the electrode bearing hm-chitosan. A zoomed-in image of a 'hot-spot' shows an intact GUV of *ca.* 20 μm diameter.

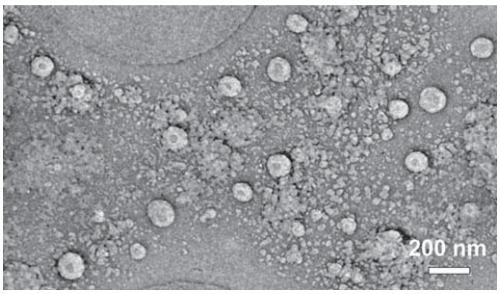

Fig. 6 Cryo-TEM image of vesicles on an hm-chitosan film. The hm-chitosan was deposited on the TEM grid and then used to capture surfactant vesicles from solution. The image shows numerous spherical objects of ~100–150 nm diameter, which are presumably intact vesicles.

vesicles and they all seem whole—no breaks or holes can be found on the vesicle shells. Thus, once again, the vesicles appear to have been captured intact.

Lastly, we present indirect functional evidence for the intactness of captured vesicles. In this experiment, we prepared liposomes containing the hydrophilic dye CF. We ensured that the dye was present only inside liposomal cores; free (unencapsulated) dye was removed *via* size-exclusion chromatography, as described in the Experimental section. The biopolymers were left untagged for this experiment to avoid overlap with the green fluorescence from the CF. Again, hm-chitosan was deposited on the left electrode and chitosan on the right. The chip was then incubated with the CF-filled liposomes followed by rinsing with DI water. At this stage, Fig. 7a shows a strong green signal only on the hm-chitosan side, implying that the liposomes preferentially attached there. The only alternate explanation is that the fluorescence comes from free CF dye stuck to the hm-chitosan, *i.e.*, that the liposomes had already been disrupted. To rule out this possibility, we added the detergent Triton X-100 into the solution above the chip. This detergent is known for its ability to disrupt liposomes into mixed micelles, whereupon dye in the liposomal cores would be released into the solution (this is illustrated by the schematics in Fig. 7). After detergent addition and subsequent rinsing, Fig. 7b shows that the green signal has vanished from the hm-chitosan film. The loss of signal after detergent treatment necessarily implies that the liposomes were initially *intact* on the hm-chitosan surface in Fig. 7a.

Spatial control of vesicle capture

We now demonstrate the capability to create specific microscale patterns of vesicles on the chip. Towards this end, we used two 6-electrode chips with a view towards engineering two specific patterns of vesicles. On one chip we deposited hm-chitosan (H) and unmodified chitosan (C) in an alternating pattern, *i.e.*, HCHCHC, on the 6 electrodes (Fig. 8a). After incubating the film with a solution of DiI-tagged surfactant vesicles, the red signal indicative of vesicles is observed *only* on the hm-chitosan (H) electrodes (Fig. 8b). Next, on the other chip, we deposited the polymers in an 'outside–inside' pattern, *i.e.*, HCHHCH (Fig. 8c). Incubation of the chip with the same tagged vesicles again results in a red signal *only* on the hm-chitosan (H) electrodes (Fig. 8d). Thus, in both cases, pre-determined patterns of vesicles were successfully created. Such patterning can be easily extended to

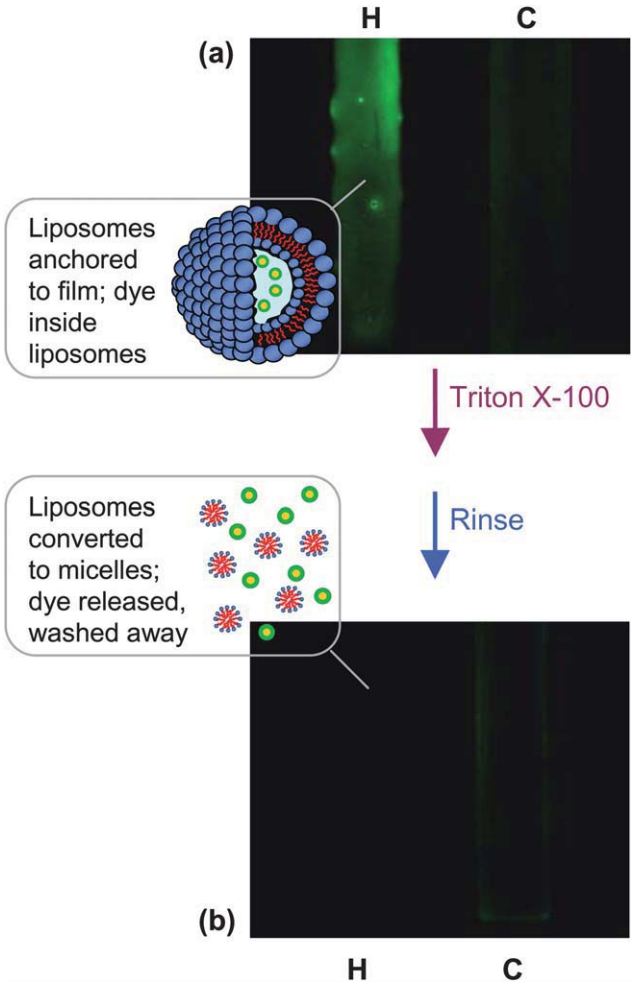

Fig. 7 Evidence for capture of intact liposomes on hm-chitosan films. (a) Green-filtered fluorescence image showing preferential binding of liposomes (filled with the hydrophilic dye CF) to the hm-chitosan (H) side relative to the chitosan (C) side. The chip is then exposed to the detergent Triton X-100 and rinsed. The detergent disrupts the liposomes into micelles, as shown by the schematics, and the encapsulated dye is thus released and washed away. (b) Fluorescence image of the rinsed chip shows nearly complete loss of fluorescent signal, confirming disruption of originally intact liposomes.

more complex designs and with finer resolution. Previous work with chitosan has indicated the resolution limits of electrodeposition to be on the order of 1 μm.[20] We view this work as a step towards the construction of "vesicle arrays" that could prove to be a useful tool for probing the properties of biomolecules such as membrane proteins.

Accessibility of captured vesicles

Lastly, for immobilized vesicles to be useful in biosensing or binding assays, the vesicles should be able to access ligands from the external solution. To evaluate this aspect, we studied the interaction between surface-bound biotinylated liposomes and streptavidin in the surrounding solution. The experiment is depicted schematically in Fig. 9a. Biotinylated liposomes were prepared by combining PC and PE–biotin in a molar ratio of 9 : 1. These liposomes were then contacted with a chip bearing hm-chitosan (H) and chitosan (C) films on adjacent electrodes. The chip was then rinsed with DI water and exposed to a solution containing fluorescently tagged streptavidin, a protein that non-covalently binds to biotin with extremely high affinity. Following a second rinsing, the results (Fig. 9b) show a significantly higher fluorescent signal from streptavidin on the hm-chitosan electrode than the chitosan electrode. The signals are quantified in the plot shown in Fig. 9c: the fluorescence is approximately 6 times higher on the hm-chitosan side (9.3 ± 0.8 gray value) relative to the chitosan side (1.6 ± 0.3 gray value). The high signal on the hm-chitosan side is evidently due to the binding of streptavidin to the biotinylated liposomes captured on that film. The binding of streptavidin to the chitosan side is not zero presumably because streptavidin (a negatively charged protein) can bind non-specifically to the positively charged chitosan, although most of these proteins are removed in the rinsing step. In sum, this is an encouraging result because it does confirm the ability of immobilized vesicles to sense reporter molecules from the surrounding environment.

4. Conclusions

We have shown that vesicles and liposomes can be captured on electrodeposited films of hm-chitosan. hm-Chitosan is

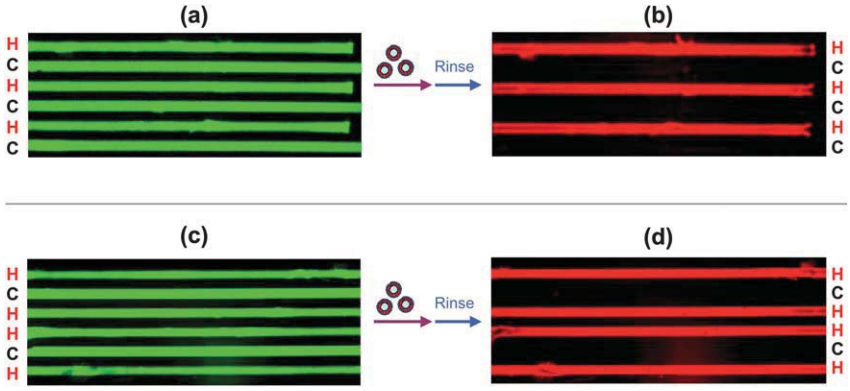

Fig. 8 Patterning of vesicles on 6-electrode chips. (a) NHS-tagged hm-chitosan (H) and chitosan (C) are electrodeposited in an alternating pattern, HCHCHC. (b) Following contact with DiI-tagged surfactant vesicles and rinsing, the red fluorescence indicative of vesicles is found only on the H electrodes. (c) H and C are electrodeposited in an 'outside–inside' pattern, HCHHCH. (d) Once again, DiI-tagged surfactant vesicles are found anchored only on the H electrodes.

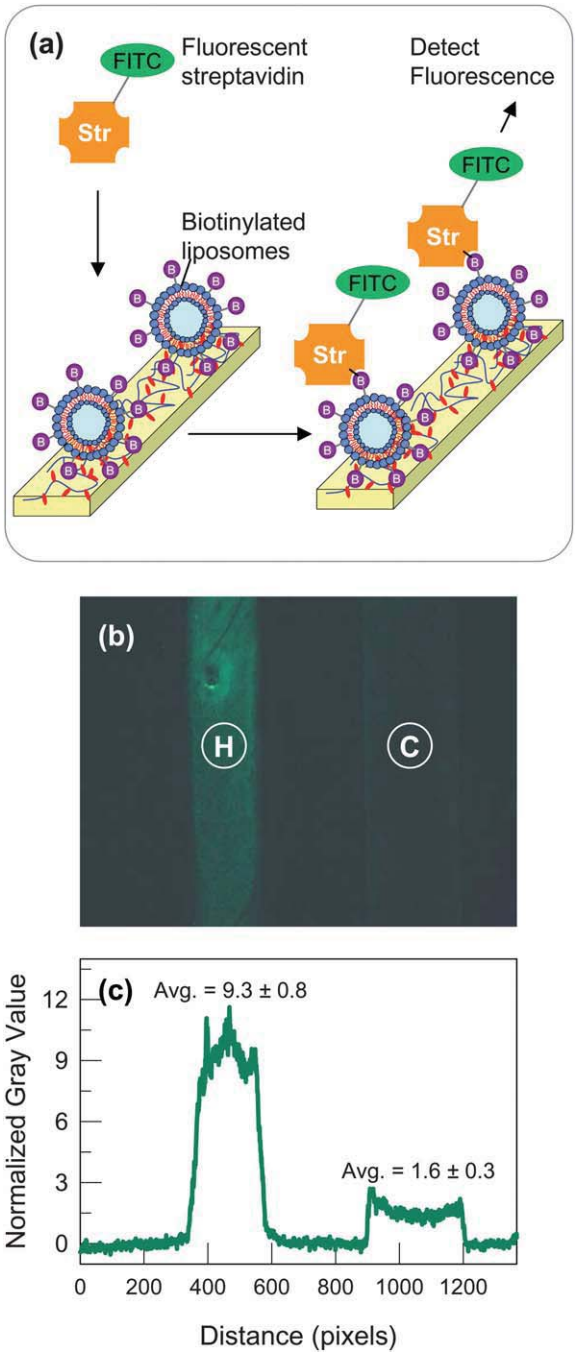

Fig. 9 Protein sensing *via* vesicles anchored to an hm-chitosan film. (a) Schematic of the experiment: biotin-decorated liposomes are first immobilized, then the chip is contacted with the fluorescently labeled protein, FITC-streptavidin. The binding of the protein is then detected by fluorescence microscopy. (b) Fluorescence image showing a strong signal from the hm-chitosan (H) electrode compared to the chitosan (C) electrode. The strong signal is indicative of protein binding to the biotins on the anchored liposomes. (c) Analysis of the intensities in (b). The average gray values for each electrode area are listed above the corresponding regions.

significantly superior in its capability for vesicle capture compared to unmodified chitosan, which implies that vesicle capture on hm-chitosan is promoted by the non-covalent binding of polymer hydrophobes to the hydrophobic interiors of vesicle bilayers. We have presented a range of evidence to show that the vesicles bound to hm-chitosan are intact structures. The evidence includes direct visualization of captured vesicles—by optical microscopy in the case of microscale GUVs and by cryo-TEM in the case of nanoscale vesicles. Additionally, key functional evidence for vesicle intactness comes from a study on dye-filled vesicles—upon detergent treatment, a loss of fluorescence from the film is observed, which can only be attributed to the detergent-induced disruption of intact vesicles. We have also confirmed the ability of biotinylated vesicles bound to hm-chitosan to conjugate with the protein streptavidin from the surrounding solution. A particular utility of using hm-chitosan as a "soft" interconnect between "hard" surfaces and vesicles is the prospect of creating patterns of immobilized vesicles. It is straightforward to electrodeposit hm-chitosan in a variety of predesigned patterns with micron-scale resolution; subsequently, vesicles can be readily captured on the patterned regions without the need for further chemistry (*i.e.*, solely by non-covalent hydrophobic interactions). The simplicity of this approach should make it attractive for researchers to create new biosensors and bioassays using vesicles.

Acknowledgements

We acknowledge funding through a Fischell Fellowship to MBD, from NSF grant CBET-0650650, and through a MIPS grant from Remedium Technologies Inc., LLC. We thank the Maryland NanoCenter and its NISP Lab for facilitating the cryo-TEM experiments, and the assistance of Dr Wen-An Chiou in performing these experiments. We also acknowledge the experimental assistance provided by undergraduate students Leigh Quang and Patrick Kelleher at various stages of this work.

References

1 D. D. Lasic, Novel applications of liposomes, *Trends Biotechnol.*, 1998, **16**, 307–321.
2 D. D. Lasic and D. Papahadjopoulos, Liposomes revisited, *Science*, 1995, **267**, 1275–1276.
3 S. M. Christensen and D. Stamou, Surface-based lipid vesicle reactor systems: fabrication and applications, *Soft Matter*, 2007, **3**, 828–836.
4 C. Yoshina-Ishii and S. G. Boxer, Arrays of mobile tethered vesicles on supported lipid bilayers, *J. Am. Chem. Soc.*, 2003, **125**, 3696–3697.
5 C. Yoshina-Ishii, Y. H. M. Chan, J. M. Johnson, L. A. Kung, P. Lenz and S. G. Boxer, Diffusive dynamics of vesicles tethered to a fluid supported bilayer by single-particle tracking, *Langmuir*, 2006, **22**, 5682–5689.
6 F. Hook, G. Stengel, A. B. Dahlin, A. Gunnarsson, M. P. Jonsson, P. Jonsson, E. Reimhult, L. Simonsson and S. Svedhem, Supported lipid bilayers, tethered lipid vesicles, and vesicle fusion investigated using gravimetric, plasmonic, and microscopy techniques, *Biointerphases*, 2008, **3**, FA108–FA116.
7 L. Lunelli, L. Pasquardini, C. Pederzolli, L. Vanzetti and M. Anderle, Covalently anchored lipid structures on amine-enriched polystyrene, *Langmuir*, 2005, **21**, 8338–8343.
8 S. Sofou and J. L. Thomas, Stable adhesion of phospholipid vesicles to modified gold surfaces, *Biosens. Bioelectron.*, 2003, **18**, 445–455.
9 H. Jung, J. Kim, J. Park, S. Lee, H. Lee, R. Kuboi and T. Kawai, Atomic force microscopy observation of highly arrayed phospholipid bilayer vesicle on a gold surface, *J. Biosci. Bioeng.*, 2006, **102**, 28–33.
10 L. S. Jung, J. S. Shumaker-Parry, C. T. Campbell, S. S. Yee and M. H. Gelb, Quantification of tight binding to surface-immobilized phospholipid vesicles using surface plasmon resonance: binding

constant of phospholipase A(2), *J. Am. Chem. Soc.*, 2000, **122**, 4177–4184.
11 E. Boukobza, A. Sonnenfeld and G. Haran, Immobilization in surface-tethered lipid vesicles as a new tool for single biomolecule spectroscopy, *J. Phys. Chem. B*, 2001, **105**, 12165–12170.
12 A. R. Patel and C. W. Frank, Quantitative analysis of tethered vesicle assemblies by quartz crystal microbalance with dissipation monitoring: binding dynamics and bound water content, *Langmuir*, 2006, **22**, 7587–7599.
13 M. A. Cooper, A. Hansson, S. Lofas and D. H. Williams, A vesicle capture sensor chip for kinetic analysis of interactions with membrane-bound receptors, *Anal. Biochem.*, 2000, **277**, 196–205.
14 G. Anderluh, M. Besenicar, A. Kladnik, J. H. Lakey and P. Macek, Properties of nonfused liposomes immobilized on an L1 Biacore chip and their permeabilization by a eukaryotic pore-forming toxin, *Anal. Biochem.*, 2005, **344**, 43–52.
15 W. Knoll, C. W. Frank, C. Heibel, R. Naumann, A. Offenhausser, J. Ruhe, E. K. Schmidt, W. W. Shen and A. Sinner, Functional tethered lipid bilayers, *J. Biotechnol.*, 2000, **74**, 137–158.
16 C. A. Naumann, O. Prucker, T. Lehmann, J. Ruhe, W. Knoll and C. W. Frank, The polymer-supported phospholipid bilayer: tethering as a new approach to substrate–membrane stabilization, *Biomacromolecules*, 2002, **3**, 27–35.
17 M. Tanaka and E. Sackmann, Polymer-supported membranes as models of the cell surface, *Nature*, 2005, **437**, 656–663.
18 Y. Deng, Y. Wang, B. Holtz, J. Y. Li, N. Traaseth, G. Veglia, B. J. Stottrup, R. Elde, D. Q. Pei, A. Guo and X. Y. Zhu, Fluidic and air-stable supported lipid bilayer and cell-mimicking microarrays, *J. Am. Chem. Soc.*, 2008, **130**, 6267–6271.
19 L. Q. Wu, A. P. Gadre, H. M. Yi, M. J. Kastantin, G. W. Rubloff, W. E. Bentley, G. F. Payne and R. Ghodssi, Voltage-dependent assembly of the polysaccharide chitosan onto an electrode surface, *Langmuir*, 2002, **18**, 8620–8625.
20 L. Q. Wu, H. M. Yi, S. Li, G. W. Rubloff, W. E. Bentley, R. Ghodssi and G. F. Payne, Spatially selective deposition of a reactive polysaccharide layer onto a patterned template, *Langmuir*, 2003, **19**, 519–524.
21 R. Fernandes, L. Q. Wu, T. H. Chen, H. M. Yi, G. W. Rubloff, R. Ghodssi, W. E. Bentley and G. F. Payne, Electrochemically induced deposition of a polysaccharide hydrogel onto a patterned surface, *Langmuir*, 2003, **19**, 4058–4062.
22 G. F. Payne and S. R. Raghavan, Chitosan: a soft interconnect for hierarchical assembly of nano-scale components, *Soft Matter*, 2007, **3**, 521–527.
23 J. H. Lee, J. P. Gustin, T. H. Chen, G. F. Payne and S. R. Raghavan, Vesicle–biopolymer gels: networks of surfactant vesicles connected by associating biopolymers, *Langmuir*, 2005, **21**, 26–33.
24 J. H. Lee, V. Agarwal, A. Bose, G. F. Payne and S. R. Raghavan, Transition from unilamellar to bilamellar vesicles induced by an amphiphilic biopolymer, *Phys. Rev. Lett.*, 2006, **96**, 048102.
25 C. Zhu, J. H. Lee, S. R. Raghavan and G. F. Payne, Bioinspired vesicle restraint and mobilization using a biopolymer scaffold, *Langmuir*, 2006, **22**, 2951–2955.
26 C. Zhu, L. Q. Wu, X. Wang, J. H. Lee, D. S. English, R. Ghodssi, S. R. Raghavan and G. F. Payne, Reversible vesicle restraint in response to spatiotemporally controlled electrical signals: a bridge between electrical and chemical signaling modes, *Langmuir*, 2007, **23**, 286–291.
27 H. Li, J. H. An, J. S. Park and K. Han, Multivesicular liposomes for oral delivery of recombinant human epidermal growth factor, *Arch. Pharmacal Res.*, 2005, **28**, 988–994.
28 J. Desbrieres, C. Martinez and M. Rinaudo, Hydrophobic derivatives of chitosan: characterization and rheological behaviour, *Int. J. Biol. Macromol.*, 1996, **19**, 21–28.
29 A. L. Kjoniksen, C. Iversen, B. Nystrom, T. Nakken and O. Palmgren, Light scattering study of semidilute aqueous systems of chitosan and hydrophobically modified chitosans, *Macromolecules*, 1998, **31**, 8142–8148.
30 C. Esquenet, P. Terech, F. Boue and E. Buhler, Structural and rheological properties of hydrophobically modified polysaccharide associative networks, *Langmuir*, 2004, **20**, 3583–3592.
31 E. W. Kaler, A. K. Murthy, B. E. Rodriguez and J. A. N. Zasadzinski, Spontaneous vesicle formation in aqueous mixtures of single-tailed surfactants, *Science*, 1989, **245**, 1371–1374.
32 E. W. Kaler, K. L. Herrington, A. K. Murthy and J. A. N. Zasadzinski, Phase-behavior and structures of mixtures of anionic and cationic surfactants, *J. Phys. Chem.*, 1992, **96**, 6698–6707.
33 M. I. Angelova and D. S. Dimitrov, Liposome electroformation, *Faraday Discuss. Chem. Soc.*, 1986, **81**, 303–306.
34 L. Mathivet, S. Cribier and P. F. Devaux, Shape change and physical properties of giant phospholipid vesicles prepared in the presence of an AC electric field, *Biophys. J.*, 1996, **70**, 1112–1121.

